

Abstract

All eddy-covariance flux measurements are associated with random uncertainties which are a combination of sampling error due to natural variability in turbulence and sensor noise. The former is the principal error for systems where the signal-to-noise ratio of the analyser is high, as is usually the case when measuring fluxes of heat, CO₂ or H₂O. Where signal is limited, which is often the case for measurements of other trace gases and aerosols, instrument uncertainties dominate. We are here applying a consistent approach based on auto- and cross-covariance functions to quantifying the total random flux error and the random error due to instrument noise separately. As with previous approaches, the random error quantification assumes that the time-lag between wind and concentration measurement is known. However, if combined with commonly used automated methods that identify the individual time-lag by looking for the maximum in the cross-covariance function of the two entities, analyser noise additionally leads to a systematic bias in the fluxes. Combining datasets from several analysers and using simulations we show that the method of time-lag determination becomes increasingly important as the magnitude of the instrument error approaches that of the sampling error. The flux bias can be particularly significant for disjunct data, whereas using a prescribed time-lag eliminates these effects (provided the time-lag does not fluctuate unduly over time). We also demonstrate that when sampling at higher elevations, where low frequency turbulence dominates and covariance peaks are broader, both the probability and magnitude of bias are magnified. We show that the statistical significance of noisy flux data can be increased (limit of detection can be decreased) by appropriate averaging of individual fluxes, but only if systematic biases are avoided by using a prescribed time-lag. Finally, we make recommendations for the analysis and reporting of data with low signal-to-noise and their associated errors.

Eddy-covariance data with low signal-to-noise ratio

B. Langford et al.

Title Page

Abstract

Introduction

Conclusions

References

Tables

Figures



Back

Close

Full Screen / Esc

Printer-friendly Version

Interactive Discussion



1 Introduction

1.1 Motivation

Surface layer fluxes of gases such as carbon dioxide (CO_2) and methane (CH_4) are frequently determined using the eddy covariance (EC) technique. This approach has allowed direct measurements of canopy-scale emission/deposition rates which are routinely incorporated into models of the carbon cycle and atmospheric chemistry. As with all measurements, the reported flux has an associated error, which should reflect both the systematic and random uncertainties of the measurement system. Systematic uncertainties arise e.g. from having an imperfect measurement system. For example, bandwidth limitations confine our ability to capture all the turbulent motions that contribute to the flux, and if uncorrected will introduce a bias. Another obvious systematic error is introduced by the uncertainty in the calibration standard. Identifying, minimizing and correcting sources of systematic bias in flux measurements remains an active area of research (Businger, 1986; Lenschow and Raupach, 1991; Lenschow et al., 1994; Mann and Lenschow, 1994; Massman, 2000; Massman and Lee., 2002). In contrast, random errors do not bias the flux but reduce the overall confidence in an individual reported value. The main sources of random uncertainties in EC flux measurements are widely accepted as (i) the stochastic nature of turbulence sampling and (ii) instrument noise and the resolution at which samples are recorded. Numerous studies have focused on quantifying random uncertainties, ranging from rigorous theoretical investigations (Lenschow and Kristensen, 1985) to more practical approaches (Hollinger and Richardson, 2005). Usually these studies have addressed the problem from the perspective of an analytical system with good signal-to-noise ratio (SNR) e.g. fluxes of sensible heat, CO_2 or H_2O , because for these measurements the uncertainty in the flux is typically dominated by natural turbulence variability. For example, Maunder et al. (2013) demonstrated that for fluxes of CO_2 and H_2O , the uncertainty associated with sensor noise was on the order of 1 % as opposed to stochastic errors which ranged between 20–30 %.

Eddy-covariance data with low signal-to-noise ratio

B. Langford et al.

Title Page

Abstract

Introduction

Conclusions

References

Tables

Figures



Back

Close

Full Screen / Esc

Printer-friendly Version

Interactive Discussion



Eddy-covariance data with low signal-to-noise ratio

B. Langford et al.

Title Page

Abstract

Introduction

Conclusions

References

Tables

Figures



Back

Close

Full Screen / Esc

Printer-friendly Version

Interactive Discussion



Increasingly, eddy-covariance is now being applied to measure fluxes of pollutants which are more difficult to measure precisely. Examples include measurements of volatile organic compounds (VOCs) (Karl et al., 2002; Langford et al., 2010; Park et al., 2013), ozone (O_3) (Coyle et al., 2009; Muller et al., 2009; Stella et al., 2013), nitric oxide (NO) (Rummel et al., 2002), nitrogen dioxide (NO_2) (Stella et al., 2013), nitrous oxide (N_2O) (Eugster et al., 2007; Famulari et al., 2010; Jones et al., 2011) and aerosols (Nemitz et al., 2008; Ahlm et al., 2009; Farmer et al., 2011, 2013). Measuring these scalars at a rate sufficient to meet the requirements for eddy covariance (i.e. several Hz) often results in a low SNR and increases the overall uncertainty in the flux.

In addition, for many of these systems, co-location of anemometer and sensor is not possible. Closed path sensors require inlet lines that create a time-lag between the vertical wind velocities (w) and measured scalar concentrations (c). Correcting phase shifts between w and c is a key step in the calculation of fluxes and is routinely done by assessing the cross-covariance function between c and w which should reveal a maximum (in absolute terms), when the data are fully synchronised. Yet, when the random uncertainty is high, as is the case for many of these analysers, the cross-covariance becomes noisy, confounding the identification of a clear maximum. Through this data treatment, the low SNR in the concentration measurement, although a random error, may effectively introduce a systematic bias towards more extreme flux values. Recently, Taipale et al. (2010) reviewed the various options for determining time-lags with reference to VOC fluxes which often have low SNR. Three commonly used approaches are the maximum (MAX), average (AVG) and prescribed (PRES) methods, which are all well suited for the automated post-processing of eddy covariance data. Briefly, the PRES method involves using a constant time-lag, predicted on the basis of the physical characteristics of the sampling system, i.e. sample flow rate and inner diameter and length of the inlet. The MAX method systematically searches for the absolute maximum value in the cross-covariance function between w and c within a pre-defined time window. Finally, the AVG method proposed by Taipale et al. (2010) applies a centred running mean to the cross-covariance function and then selects the flux from the

**Eddy-covariance data
with low
signal-to-noise ratio**B. Langford et al.

[Title Page](#)[Abstract](#)[Introduction](#)[Conclusions](#)[References](#)[Tables](#)[Figures](#)[Back](#)[Close](#)[Full Screen / Esc](#)[Printer-friendly Version](#)[Interactive Discussion](#)

unsmoothed cross-covariance function that corresponds to the maximum of the absolute running mean. The latter method was originally developed for use with VOC data measured by proton transfer reaction mass spectrometer (PTR-MS), but is generically applicable to any dataset with low SNR. There are currently no guidelines on the degree of smoothing that should be applied (i.e. the length of the running mean). In their study, Taipale et al. (2010) settle on a five second running mean, recognising that this is an arbitrary length.

With so many options available, it is clear that the calculated flux may differ depending on the chosen time-lag method. For example, in their study Taipale et al. (2010) confirm that using a prescribed time-lag may result in a systematic underestimation of the flux as the “true” time-lag is likely to vary over time due to fluctuations in pumping speed but also due to the degree of absorption/desorption with the inlet wall and its effect on the effective transport time through the tube. Especially for the more water soluble compounds this may change with humidity and or the aerosol coating of the inlet. Similarly, systematically searching for a maximum within a noisy cross-covariance with multiple local maxima may well bias fluxes towards more extreme values (Laurila et al., 2012). The AVG method offers something of a compromise between the two approaches, but some systematic bias may still remain.

We hypothesise that the bias induced by using methods that search for a maximum in the cross-covariance is closely linked to the random error in the flux, which is in part a function of the SNR of the analytical instrumentation and in some cases may be greater than the systematic error induced from using a prescribed time-lag. In order to address this hypothesis an appropriate method is needed to quantify the random error in the flux and separate it into sampling and instrument error components.

1.2 Common approaches for quantifying random flux errors

Assuming the time-lag is known, the random error of an eddy covariance flux can be estimated in a variety of ways (Lenschow and Kristensen, 1985). One traditional method is mainly used to estimate the flux error due to the limited sampling of the

stochastic nature of turbulence. It is based on the variance of the instantaneous values of $w'c'$ and the integral time scale and is estimated as (Lumley and Papanofsky, 1964; Wyngaard, 1973; Lenschow et al., 1994):

$$RE = \left[\frac{2\sigma_{w'c'}^2 \tau_{Fc}}{L} \right]^{0.5} \quad (1)$$

5 where L is the length of the averaging period in seconds, $\sigma_{w'c'}^2$ is the variance of the time-series of instantaneous values of $w'c'$ over a typical averaging period (~ 30 min) and τ_{Fc} is the integral time scale, i.e. the average time-scale over which correlation persists. The integral time scale can be directly estimated by integrating the area under the auto-covariance of $(w'c')$ to the point of first zero crossing. However, this gets
 10 more difficult for cases with high noise levels, as the auto-covariance becomes more scattered resulting in multiple zero crossings including some artificially close to the zero time-lag. This has the consequence that the integral timescale derived by this method becomes physically meaningless. In theory, additional sensor noise should increase the random error but in this case the reduction in the estimate of τ_{Fc} has the knock-on effect of minimising the error estimate. Consequently, this approach appears unsuitable
 15 in situations where signal is limited. An alternative approach, for conditions of neutral stability, is to approximate the integral time scale by dividing the measurement height (z) above the zero plane displacement (d), by the mean wind speed (\bar{u}). Yet, Rannik et al. (2009) found this method to overestimate the integral scale by a factor of two and consequently the random flux error by a factor of 1.4.
 20

Mahrt (1998) offered an alternative method that negates the use of the integral timescale by splitting the time series into sub-records and formulating the error as the standard error between sub-records (Mahrt, 1998; Rannik et al., 2009):

$$RE = \left[\frac{\sigma_{Fc.sub}^2}{n} \right]^{0.5}, \quad (2)$$

**Eddy-covariance data
with low
signal-to-noise ratio**

B. Langford et al.

Title Page	
Abstract	Introduction
Conclusions	References
Tables	Figures
◀	▶
◀	▶
Back	Close
Full Screen / Esc	
Printer-friendly Version	
Interactive Discussion	



mostly be attributed to instrument noise. This is an intriguing option, yet, if we consider a measured time series c , which is made up of some genuine signal (x) as well as instrumental noise (ε), then the effective amplitude of a time shuffled time series is still composed of $x + \varepsilon$ and therefore the uncertainty is likely overestimated.

More recently Mauder et al. (2013) approximated errors associated with random instrument noise by first calculating the signal-to-noise ratio of the analyser using an auto-covariance function and then using a basic error propagation to estimate the contribution of that noise to the uncertainty in the cross-covariance:

$$RE_{\text{noise}} = \sqrt{\frac{(\sigma_C^{\text{noise}})^2 \sigma_w^2}{N}}, \quad (3)$$

In this approach, σ_C^{noise} is the SD of the instrument noise, derived using an auto-covariance function (see Sect. 2.1 for details), σ_w^2 is the variance of the vertical wind velocity and N is the number of data points in the flux averaging period. This method, also implemented by Peltola et al. (2014) and Rannik et al. (2015) is relatively simple to apply but as yet, its effectiveness has not been fully validated for use with EC and DEC data.

In this study we explore a further possibility for estimating the portion of random error attributable to sensor noise by combining the ideas of Billesbach (2011) and Mauder et al. (2013), focusing in particular on the interplay between random instrument uncertainty, cross-covariance peak width and the systematic flux bias induced when determining the flux through the use of a cross-covariance function (Taipale et al., 2010; Laurila et al., 2012). In understanding this linkage, our aims are to (i) validate the use of Eq. (3) for use with EC and DEC data sets, (ii) outline an optimal strategy for calculating and reporting random errors and (iii) for determining time-lags for eddy covariance data with low SNR and to draw conclusions on the value of flux measurements made with low SNR.

Eddy-covariance data with low signal-to-noise ratio

B. Langford et al.

Title Page

Abstract

Introduction

Conclusions

References

Tables

Figures

◀

▶

◀

▶

Back

Close

Full Screen / Esc

Printer-friendly Version

Interactive Discussion



2 Methods

2.1 Quantifying random white noise from analysers

Instrumental noise comes in both structured and unstructured forms. For example, the 50–60 Hz signal from a mains AC power supply might introduce a structured noise into a time series, and optical fringes often introduce periodic features in optical spectroscopic approaches. By contrast, uncorrelated white noise can result from minor fluctuations in the mechanics of instrument components, or fluctuations in temperature, pressure or humidity. Here we focus our attention on unstructured, white noise only, and define the SNR for a given time series c as:

$$\text{SNR} = \frac{\sigma_{x'}^2}{\sigma_{\varepsilon}^2}, \quad (4)$$

where $\sigma_{x'}^2$ is the variance of the genuine signal of a measured timeseries, c ($c = x + \varepsilon$, where x is genuine signal and ε is noise) and σ_{ε}^2 is the variance of the noise. In order to establish the relative contributions of both signal and noise components of c we apply an auto-covariance to c' of the form:

$$\text{AC}_{(\tau)} = \overline{(x'_t + \varepsilon_t)(x'_{t+\tau} + \varepsilon_{t+\tau})}, \quad (5)$$

where τ is the time-lag (in number of data points or sampling intervals) and primes denote fluctuations about the mean. White noise can only contribute to the auto-covariance at $\tau = 0$ (Lenschow et al., 2000; Maunder et al., 2013) as it has no structure (i.e. the noise on an individual data point is uncorrelated to the noise of the adjacent data points). As the auto-covariance function moves away from zero, the contribution of instrument white noise is removed and thus the difference between $\text{AC}_{(0)}$ and $\text{AC}_{(1)}$ gives an estimate of random instrument noise. The underlying trend in the auto-covariance function of the genuine signal depends on the biophysical (source/sink

Title Page

Abstract

Introduction

Conclusions

References

Tables

Figures



Back

Close

Full Screen / Esc

Printer-friendly Version

Interactive Discussion



Eddy-covariance data with low signal-to-noise ratio

B. Langford et al.

Title Page

Abstract

Introduction

Conclusions

References

Tables

Figures



Back

Close

Full Screen / Esc

Printer-friendly Version

Interactive Discussion



strength) signature of the compound being measured, and the structure within the turbulence signal which is itself a function of atmospheric stability. The presence of a trend or “structure” in the auto-covariance is a sign of genuine signal in the data, whereas an auto-covariance with no underlying trend is the definition of white noise. Where a genuine signal is present it is therefore necessary to extrapolate the positive auto-covariance function back to the zero point. This is typically done using only the first few points e.g. $AC_{(1-5)}$. The noise can then be estimated as the difference between $AC_{(0)}$ and $AC_{(1-5 \text{ extrapolated})}$ and is depicted in Fig. 1a. In some cases the auto-covariance decreases exponentially and therefore it is appropriate to fit these points using an exponential extrapolation as opposed to the linear fit depicted in Fig. 1 and used throughout this study.

Using the auto-covariance function as opposed to the auto-correlation function means the calculated signal and noise are variances and retain their original units. Taking the square root gives the SD of both the signal and noise components.

The auto-covariance is a convenient method when working in the time domain, but alternatives are available when analysing the data in the frequency domain. Figure 1b shows the variance spectrum for $w'T'$. The red line shows the spectra of unmodified temperature data from an ultrasonic anemometer and the blue line shows the same temperature data deteriorated through the addition of Gaussian white noise with a SD of 1 K. In the frequency domain, on this plot, the fall-off towards higher frequencies in the inertial sub-range should follow a $-5/3$ slope, while white noise follows a $+1$ slope. This enables the noise variance to be quantified as the area between solid and dashed lines in Fig. 1b, although, visually, the area becomes proportional to the noise variance only on a log-linear plot as opposed to the log-log depiction shown here (Stull, 1988). It should be noted that the auto-covariance method is unsuitable if the measured time series (c) is not used with the original time resolution, e.g. if it was first re-sampled to a different sampling frequency in order to match the sonic time resolution. Similarly, this technique does not apply to structured noise, because $AC_{(1)}$ would still be affected

by such noise. In the auto-covariance approach, structured noise may or may not show up as a departure from the $-5/3$ slope at high frequencies.

Throughout this paper we utilise the auto-covariance method in the time domain as it is readily applicable to both eddy covariance and disjunct eddy covariance (DEC) datasets.

2.2 Quantifying random flux errors and the limit of detection

As discussed previously, the precision with which a flux can be measured is commonly approximated from the properties of the cross-covariance function between w' and c' ($f_{w'c'}$). For time-lags τ much different from the true time-lag, the SD of $f_{w'c'}(\tau)$ provides a measure of the random error affecting the flux (1995; Spirig et al., 2005). Multiplying this value ($\sigma_{f_{w'c'}} \times 3$) gives an estimate of the measurement precision at the 99th confidence intervals which can be used as the flux limit of detection (LoD). This threshold does not only depend on the SNR of the concentration measurement, but also varies with wind speed and atmospheric stability. Therefore, for each new averaging period it is necessary to recalculate the LoD. Whilst this technique allows for the separation of a “genuine” flux signature from the general noise of the covariance, the determination of the SD is often done using somewhat arbitrary boundaries (e.g. -150 to 180 and $+150$ to 180 s, or defined as some multiple of the integral timescale, Spirig et al., 2005), and thus as the turbulence structure evolves throughout the day, these limits may become more or less appropriate. Any correlation between c' and w' within these bounds is either purely accidental and reflects the random noise in the time-series or it is due to organised structures that persist over much longer time intervals suggesting that turbulence is not stationary or statistically not well covered in the measurement. Furthermore, a trend in scalar data can result in a cross-covariance which remains positive or negative over wide ranges rather than the expected fluctuation around zero. Figure 2a and b shows the calculation of the LoD via the SD (LoD (Wienhold/Spirig; blue dashed line) to sensible heat flux data from a forest site, for cases where the cross-covariance oscillates around zero and is offset from zero, respectively. In the lat-

Eddy-covariance data with low signal-to-noise ratio

B. Langford et al.

Title Page

Abstract

Introduction

Conclusions

References

Tables

Figures



Back

Close

Full Screen / Esc

Printer-friendly Version

Interactive Discussion



ter case (Fig. 2b) many points of the cross-covariance function lie outside the limit of detection.

A modification of the $\sigma_{f_{w'c'}}$ approach is to use the root mean squared deviation (RMS) of $f_{w'c'}$ from zero within the same specified region (greyed area – Fig. 2a and b), which reflects the variability in the cross-covariance function in these regions, but also its offset from zero. Figure 2c shows the LoD for sensible heat flux data calculated using both the $\text{RMS}_{f_{w'c'}}$ and $\sigma_{f_{w'c'}}$ methods. The two methods agree very closely for periods where the cross-covariance fluctuates regularly around zero as in Fig. 2a, but where the covariance is predominantly of one sign the SD approach derives significantly smaller limits of detection, which we believe to be underestimates of the true uncertainty. Importantly, using linear detrending of the scalar data as opposed to block averaging reduces this effect but does not completely remove it. For this data set, 14 % of block averaged data would have been rejected using the LoD based on $\text{RMS}_{f_{w'c'}}$ as opposed to 4 % using the traditional $\sigma_{f_{w'c'}}$ method. In contrast, when applying linear detrending to these data the percentage of data rejected fall to 6 and 3 % for the $\text{RMS}_{f_{w'c'}}$ and the $\sigma_{f_{w'c'}}$ methods, respectively. In light of these findings we utilise the $\text{RMS}_{f_{w'c'}}$ method for all calculations of the flux LoD in this study. Recommendations for the application of the RMS method to ozone eddy-covariance flux data are outlined in Nemitz et al. (2015).

2.3 Calculating the effect of instrument noise on the flux error

Analysis of the statistical properties of the cross-covariance function seems to offer a practical approach for approximating the total random error of the flux, because the variability of the cross-covariance function comprises both instrument noise and the variability of the (genuine) atmospheric concentration. Yet, as discussed above, isolating the instrumental component of the total random error remains a challenge. Here, we attempt to untangle the two errors using an approach similar to the “random shuffle” method of Billesbach (2011). Rather than shuffling the measured scalar time series to remove any covariance between c' and w' , we generate a new time series of equal length comprised purely of Gaussian white noise. The SD of the white noise

Eddy-covariance data with low signal-to-noise ratio

B. Langford et al.

Title Page

Abstract

Introduction

Conclusions

References

Tables

Figures



Back

Close

Full Screen / Esc

Printer-friendly Version

Interactive Discussion



Eddy-covariance data with low signal-to-noise ratio

B. Langford et al.

Title Page

Abstract

Introduction

Conclusions

References

Tables

Figures



Back

Close

Full Screen / Esc

Printer-friendly Version

Interactive Discussion



is set to match that of the instrument noise, ε' , which can be calculated using the auto-covariance method described in Sect. 2.1. The resulting time series shares the statistical properties of c' , minus the contribution of the genuine analyser signal x' and therefore the effect of the instrument error on the flux error can now be calculated by

5 applying the RMS method to the cross-covariance of $f_{w'}\varepsilon'$.

The six steps of this method are summarised as follows:

1. Perform an auto-covariance of the scalar prime c' to obtain the SD of the instrument noise ε' .
2. Generate a time series of white noise with a SD matching that of the instrument
- 10 noise.
3. Calculate the cross-covariance $f_{w'}c'$.
4. Calculate the cross-covariance $f_{w'}\varepsilon'$.
5. Apply RMS method to $f_{w'}c'$ to obtain total random error (RE).
6. Apply RMS method to $f_{w'}\varepsilon'$ to obtain Instrumental random error (RE_{noise}).

15 In theory this numerical exercise seeks to quantify the same error approximated by Maunder et al. (2013) (Eq. 3), whilst making no assumptions on the shape of the distribution of w' . Therefore we can use this approach to validate Eq. (3) for use with both EC and DEC data sets and assess its performance when applied to data sets with varying levels of SNR. The random instrument errors calculated using both these

20 approaches are compared in Sect. 3.1.

Although this proposed technique does not make any assumption about the distribution of w' , it does make the assumption that the instrument noise follows a Gaussian distribution which is not always the case. For example, concentrations have often been found to be skewed towards larger values. In particular, tracers which show a high degree of variability at low mean concentrations may be log-normally distributed: concentrations are not constrained towards larger values, but cannot physically be negative.

25

**Eddy-covariance data
with low
signal-to-noise ratio**

B. Langford et al.

[Title Page](#)[Abstract](#)[Introduction](#)[Conclusions](#)[References](#)[Tables](#)[Figures](#)[Back](#)[Close](#)[Full Screen / Esc](#)[Printer-friendly Version](#)[Interactive Discussion](#)

The combined frequency distribution of w' and c' has been found to be more closely approximated by a Gram–Charlier equation than a Gaussian distribution (Milne et al., 2001). In addition, the statistical noise generated by instruments that derive concentrations from count events, e.g. counting particle number, ions (as the PTR-MS does for VOC fluxes or the Aerosol Mass Spectrometer for submicron aerosol chemical fluxes), follows a Poisson distribution, which at low concentrations may act on the flux in a different way to a normally distributed instrument noise.

With this in mind we performed several tests to determine if the covariance between the vertical wind velocity and a time series of white noise is sensitive to the distribution of the noise selected. For a single 30 min averaging period the covariance was calculated between w' and ε' whereby the artificially generated noise (ε') was either Gaussian, Poisson or log normally distributed as seen in Fig. 3a. The white noise flux for the same averaging period was repeatedly calculated, using a prescribed time-lag, for 5000 artificially generated time-series each, and the resulting distributions are shown in Fig. 3b. All three white noise distribution types are evenly distributed about zero, which demonstrates that unstructured white noise creates a random uncertainty in the flux but does not induce a systematic bias, regardless of its distribution. These findings provide assurances for eddy covariance systems that induce a Poisson counting noise that flux biases are not created.

These findings confirm the theoretical considerations of Lenchow and Kristensen (1985), that, if the time-lag is known, the presence of uncorrelated noise induces a random uncertainty in the flux but does not induce a systematic bias. Nonetheless, this conclusion does not consider the interplay of this noise with the determination of a time lag, which is vital for sensors that are spatially separated from the vertical wind velocity measurement, and its potential to introduce a bias that is a function of the random error.

2.4 Effect of instrument noise on time-lag determination

2.4.1 Signal-to-noise simulations

In order to investigate the influence of unstructured white noise from analysers and the method of time-lag determination on calculated fluxes, a series of simulations were performed using 31 days of sensible heat flux data (see Supplement). Time-lags were determined using the three main methods outlined above, MAX, AVG and PRES. For the AVG method, a further ten scenarios were implemented, whereby the running mean applied to the cross-covariance was increased from 0.5 to 5 s in 0.5 s intervals. In all scenarios the time-lag was sought within a 10 s window which ranged from -5 to $+5$ s, with the true time-lag obviously being 0 s. For the AVG method, the running mean was applied over a larger window to ensure the mean was properly centred for all data in the 10 s window. To accurately control the analyser noise level, the SNR of the temperature data was first quantified using the auto-covariance approach outlined above. The signal was then deteriorated by adding Gaussian white noise until a target signal-to-noise ratio was achieved to within a 1 % tolerance. Sensible heat fluxes were calculated using block averaging and a reference flux was determined by calculating the flux with zero lag from the un-manipulated temperature time series. This process was repeated ten times for temperature data with a signal-to-noise ratio (SNR^{-1}) ranging between 200 and 0.05. In addition, the above simulation was repeated three more times to assess the impact of adopting disjunct sampling protocols of 2.5, 5 and 7.5 s as is common for measurements of VOC fluxes by PTR-MS and aerosol fluxes by Q-AMS. The overall bias between simulated time series and the reference was determined by the gradient of the regression between 31 days of reference data vs. those of the simulations.

2.4.2 Peak width simulation

The covariance between the genuine signals of c' (e.g. x') and w' gives a peak with respect to time-lag in the cross-covariance function. Superimposed on top of this peak

AMTD

8, 2913–2955, 2015

Eddy-covariance data with low signal-to-noise ratio

B. Langford et al.

Title Page

Abstract

Introduction

Conclusions

References

Tables

Figures



Back

Close

Full Screen / Esc

Printer-friendly Version

Interactive Discussion



3.2 Bias effects of different time-lag determination methods

3.2.1 Dependence on signal-to-noise ratio

The simulations applied to sensible heat flux data reveal a distinct relationship between the signal-to-noise ratio of the analyser and the relative flux bias for both the MAX and AVG lag determination methods. Figure 6 shows the results for 10 Hz eddy covariance data. It is immediately apparent that methods that systematically search for a maximum (red trace) induce an average positive bias (towards more extreme emission or deposition) to the reported flux which increases exponentially as the analyser signal deteriorates. For this dataset, the relative bias can be as much as 18%. Adopting the AVG method can significantly reduce this error provided the applied running mean is of a suitable length. However, selection of an inappropriate running mean may allow the bias to persist and can also become negative when overly long. The reason for the negative lies in the fact that the shape of the peak in the covariance spectrum tends to be skewed, while the running average of the AVE peak fit is symmetrical. However, theory cannot currently explain the skewness which is therefore difficult to predict. By contrast, the use of a fixed time-lag (for the anemometer temperature data the time-lag is known to be zero), uncertainty increases as the signal is more and more deteriorated, but to a smaller degree, and its sign is random.

Figure 7 shows the same set of simulations for data that have disjunct sampling intervals of 2.5 (Fig. 7a), 5 (Fig. 7b) and 7.5 (Fig. 7c) seconds. It is well understood that adopting a disjunct sampling approach reduces the statistical sample size and thus increases the random error (Lenschow et al., 1994; Rinne and Ammann, 2012). However, it is frequently assumed that the increased random error does not translate to a systematic bias in the measured fluxes, but our simulations show this not to be the case. The poor sampling statistics and high instrument noise combined with the MAX method for time-lag identification can potentially lead to 100 or even 200% overestimation in the mean flux.

Eddy-covariance data with low signal-to-noise ratio

B. Langford et al.

Title Page

Abstract

Introduction

Conclusions

References

Tables

Figures



Back

Close

Full Screen / Esc

Printer-friendly Version

Interactive Discussion



that the FWHM maximum of the covariance peak is an equally important parameter. Broader covariance peaks result in a higher probability of an extreme maximum being chosen and therefore both the probability of overestimating the flux and the magnitude of the bias are closely linked to the peak width. The logarithmic relationship between turbulence and height mean trace gas and aerosol flux measurements at higher elevations above ground are more at risk to systematic bias when the MAX or AVG methods are employed. Conversely, the probability of systematic underestimation of the flux through the use of a prescribed time-lag at these measurement heights is somewhat reduced due to a greater tolerance afforded by the increased peak width. Massman (2000) and Hörtnagl et al. (2010) recognised that further broadening of the covariance peak is possible through the attenuation of scalars through long inlet lines and also through an increase in the analyser integration time. Therefore, when working on tall towers above forests or urban canopies one should be aware of the greater potential for systematic bias and should consider the use of a prescribed time-lag which may provide the most representative (least biased) estimate of the flux. In general terms, when sampling at lower heights such as above crops or grassland, the potential for bias is lessened, whereas the likelihood of underestimating the flux through the use of a prescribed time-lag is increased. Nonetheless, during more unstable periods the potential for a greater influence of lower frequencies in the turbulence spectra cannot be overlooked (Horst, 2000).

When using a prescribed time-lag the attenuation of samples through long inlet lines, adsorption/desorption effects and fluctuations in pump flow rate are not typically considered. More often, the prescribed value is chosen purely on the basis of the inlet dimensions and a spot measurement of the flow rate, or through a single test where a pulse in concentration and wind speed is created near the anemometer/inlet. In these cases the potential for underestimating the flux is large. It is therefore good practice to initially search for the time-lag using the AVG or MAX method and to plot the results as a histogram or time series. This may confirm that the time-lag was indeed constant or it may reveal a clear peak or trend in time-lags which can be used to set the prescribed

**Eddy-covariance data
with low
signal-to-noise ratio**

B. Langford et al.

Title Page

Abstract

Introduction

Conclusions

References

Tables

Figures



Back

Close

Full Screen / Esc

Printer-friendly Version

Interactive Discussion



5 a flux. Adopting the MAX or AVG methods exaggerates the mirroring by systematically choosing the furthest point away from zero which in the extreme case can result in the very unnatural flux distributions shown in Fig. 10. Adopting the AVG method with 5 s running mean limits this effect to a certain extent, but a noticeable dip around zero remains. Importantly, the use of a prescribed time-lag eliminates the splitting of data from either side of zero to give a much more natural looking flux distribution.

10 In addition to the calculated fluxes, the red time traces show the Gaussian white noise flux (F_{GN}), i.e. the cross-covariance between an artificially generated white noise signal that shares the same SD as the analyser noise. Here, both tracer and Gaussian noise fluxes have been calculated using the MAX method. For acetone, F_{GN} is of a similar magnitude which indicates that in this example the fluxes shown are almost entirely due to coincidental covariance between the vertical wind velocity and instrument noise. In contrast, the range of benzene and particle number fluxes both at least partially exceeds the Gaussian white noise flux and show sustained period of emission fluxes indicating the presence of a “genuine” flux which is, for certain periods, distinguishable from the random sensor noise flux. The remaining data would undoubtedly fall below conventional limits of detection and the individual 30 min flux measurements would ordinarily be rejected. Yet, the question remains whether any useful information on the net exchange can still be extracted from data such as these and is discussed in detail in Sect. 3.3.2. Finally, the TDL N_2O fluxes are consistently larger than the Gaussian white noise flux despite an apparent mirroring in the data. In this case it is likely that the instrument noise is comprised of both unstructured white noise and structured noise perhaps from optical fringes which our method does not take into account. It should be noted, that we here tried to identify data series which showed the effects of limited SNR. All these instruments obviously can perform better in situations where 25 fluxes are larger or where instrumentation parameters are further optimised.

Acknowledgements. We thank the members of the ECLAIRE flux community for their useful comments and recommendations. This work was funded by the EU FP7 grant ECLAIRE (no. 282 910) and through the NERC ClearLo grant (NE/H003169/1).

References

- 5 Acton, W. J. F., Schallhart, S., Langford, B., Fares, S., Valach, A., Rantala, P., Hewitt, C. N., and Nemitz, E.: Comparison of three methods to derive canopy-scale flux measurements above a mixed oak and hornbeam forest in Northern Italy, in preparation for Atmos. Chem. Phys. Discuss., 2015.
- 10 Ahlm, L., Nilsson, E. D., Krejci, R., Mårtensson, E. M., Vogt, M., and Artaxo, P.: Aerosol number fluxes over the Amazon rain forest during the wet season, Atmos. Chem. Phys., 9, 9381–9400, doi:10.5194/acp-9-9381-2009, 2009.
- Billesbach, D. P.: Estimating uncertainties in individual eddy covariance flux measurements: a comparison of methods and a proposed new method, Agr. Forest Meteorol., 151, 394–405, 2011.
- 15 Billesbach, D. P., Kim, J., Clement, R. J., Verma, S. B., and Ullman, F. G.: An intercomparison of two tunable diode laser spectrometers used for eddy correlation measurements of methane flux in a prairie wetland, J. Atmos. Ocean. Tech., 15, 197–206, 1998.
- Businger, J. A.: Evaluation of the accuracy with which dry deposition can be measured with current micrometeorological techniques, J. Clim. Appl. Meteorol., 25, 1100–1124, 1986.
- 20 Clement, R. J., Verma, S. B., and Verry, E. S.: Relating chamber measurements to eddy-correlation measurements of methane flux, J. Geophys. Res.-Atmos., 100, 21047–21056, 1995.
- Coyle, M., Nemitz, E., Storeton-West, R., Fowler, D., and Cape, J. N.: Measurements of ozone deposition to a potato canopy, Agr. Forest Meteorol., 149, 655–666, 2009.
- 25 Eugster, W., Zeyer, K., Zeeman, M., Michna, P., Zingg, A., Buchmann, N., and Emmenegger, L.: Methodical study of nitrous oxide eddy covariance measurements using quantum cascade laser spectrometry over a Swiss forest, Biogeosciences, 4, 927–939, doi:10.5194/bg-4-927-2007, 2007.

Eddy-covariance data with low signal-to-noise ratio

B. Langford et al.

Title Page

Abstract

Introduction

Conclusions

References

Tables

Figures



Back

Close

Full Screen / Esc

Printer-friendly Version

Interactive Discussion



Eddy-covariance data with low signal-to-noise ratio

B. Langford et al.

Title Page

Abstract

Introduction

Conclusions

References

Tables

Figures



Back

Close

Full Screen / Esc

Printer-friendly Version

Interactive Discussion



Famulari, D., Nemitz, E., Di Marco, C., Phillips, G. J., Thomas, R., House, E., and Fowler, D.: Eddy-covariance measurements of nitrous oxide fluxes above a city, *Agr. Forest Meteorol.*, 150, 786–793, 2010.

Farmer, D. K., Kimmel, J. R., Phillips, G., Docherty, K. S., Worsnop, D. R., Sueper, D., Nemitz, E., and Jimenez, J. L.: Eddy covariance measurements with high-resolution time-of-flight aerosol mass spectrometry: a new approach to chemically resolved aerosol fluxes, *Atmos. Meas. Tech.*, 4, 1275–1289, doi:10.5194/amt-4-1275-2011, 2011.

Farmer, D. K., Chen, Q., Kimmel, J. R., Docherty, K. S., Nemitz, E., Artaxo, P. A., Cappa, C. D., Martin, S. T., and Jimenez, J. L.: Chemically resolved particle fluxes over tropical and temperate forests, *Aerosol Sci. Tech.*, 47, 818–830, 2013.

Hollinger, D. Y. and Richardson, A. D.: Uncertainty in eddy covariance measurements and its application to physiological models, *Tree Physiol.*, 25, 873–885, 2005.

Hörtnagl, L., Clement, R., Graus, M., Hammerle, A., Hansel, A., and Wohlfahrt, G.: Dealing with disjunct concentration measurements in eddy covariance applications: a comparison of available approaches, *Atmos. Environ.*, 44, 2024–2032, 2010.

Horst, T. W.: On frequency response corrections for eddy covariance flux measurements, *Bound.-Lay. Meteorol.*, 94, 517–520, 2000.

Ibrom, A., Dellwik, E., Larsen, S. E., and Pilegaard, K.: On the use of the Webb–Pearman–Leuning theory for closed-path eddy correlation measurements, *Tellus B*, 59, 937–946, 2007.

Jones, S. K., Famulari, D., Di Marco, C. F., Nemitz, E., Skiba, U. M., Rees, R. M., and Sutton, M. A.: Nitrous oxide emissions from managed grassland: a comparison of eddy covariance and static chamber measurements, *Atmos. Meas. Tech.*, 4, 2179–2194, doi:10.5194/amt-4-2179-2011, 2011.

Karl, T. G., Spirig, C., Rinne, J., Stroud, C., Prevost, P., Greenberg, J., Fall, R., and Guenther, A.: Virtual disjunct eddy covariance measurements of organic compound fluxes from a subalpine forest using proton transfer reaction mass spectrometry, *Atmos. Chem. Phys.*, 2, 279–291, doi:10.5194/acp-2-279-2002, 2002.

Langford, B., Misztal, P. K., Nemitz, E., Davison, B., Helfter, C., Pugh, T. A. M., MacKenzie, A. R., Lim, S. F., and Hewitt, C. N.: Fluxes and concentrations of volatile organic compounds from a South-East Asian tropical rainforest, *Atmos. Chem. Phys.*, 10, 8391–8412, doi:10.5194/acp-10-8391-2010, 2010.

Laurila, T., Aurela Mand Tuovinen, J.: Eddy covariance measurements over wetlands, in: *Eddy Covariance: a Practical Guide to Measurements and Data Analysis*, edited by: Aubinet, M.,

Eddy-covariance data with low signal-to-noise ratio

B. Langford et al.

Title Page

Abstract

Introduction

Conclusions

References

Tables

Figures



Back

Close

Full Screen / Esc

Printer-friendly Version

Interactive Discussion



Vesala, T., and Papale, D., Springer, Dordrecht, Heidelberg, London, New York, 14, 345–360, 2012.

Lenschow, D. and Kristensen, L.: Uncorrelated noise in turbulence measurements, *J. Atmos. Ocean. Tech.*, 2, 68–81, 1985.

5 Lenschow, D. H. and Raupach, M. R.: The attenuation of fluctuations in scalar concentrations through sampling, *J. Geophys. Res.-Atmos.*, 96, 15259–15268, 1991.

Lenschow, D. H., Mann, J., and Kristensen, L.: How long is long enough when measuring fluxes and other turbulence statistics, *J. Atmos. Ocean. Tech.*, 11, 661–673, 1994.

10 Lenschow, D. H., Wulfmeyer, V., and Senff, C.: Measuring second- through fourth-order moments in noisy data, *J. Atmos. Ocean. Tech.*, 17, 1330–1347, 2000.

Lumley, J. L. and Panofsky, H. A.: *The Structure of Atmospheric Turbulence*, John Wiley & Sons, pp. 239, 1964.

Mahrt, L.: Flux sampling errors for aircraft and towers, *J. Atmos. Ocean. Tech.*, 15, 416–429, 1998.

15 Mann, J. and Lenschow, D. H.: Errors in airborne flux measurements, *J. Geophys. Res.-Atmos.*, 99, 14519–14526, 1994.

Massman, W. J.: A simple method for estimating frequency response corrections for eddy covariance systems, *Agr. Forest Meteorol.*, 104, 185–198, 2000.

20 Massman, W. J. and Lee, X.: Eddy covariance flux corrections and uncertainties in long-term studies of carbon and energy exchanges, *Agr. Forest Meteorol.*, 113, 121–144, 2002.

Mauder, M., Cuntz, M., Druce, C., Graf, A., Rebmann, C., Schmid, H. P., Schmidt, M., and Steinbrecher, R.: A strategy for quality and uncertainty assessment of long-term eddy-covariance measurements, *Agr. Forest Meteorol.*, 169, 122–135, 2013.

25 Milne, R., Mennim, A., and Hargreaves, K.: The value of the coefficient in the relaxed eddy accumulation method in terms of fourth order moments, *Bound.-Lay. Meteorol.*, 101, 359–373, 2001.

Muller, J. B. A., Coyle, M., Fowler, D., Gallagher, M. W., Nemitz, E. G., and Percival, C. J.: Comparison of ozone fluxes over grassland by gradient and eddy covariance technique, *Atmos. Sci. Lett.*, 10, 164–169, 2009.

30 Nemitz, E., Gallagher, M. W., Duyzer, J. H., and Fowler, D.: Micrometeorological measurements of particle deposition velocities to moorland vegetation, *Q. J. Roy. Meteor. Soc.*, 128, 2281–2300, 2002.

**Eddy-covariance data
with low
signal-to-noise ratio**

B. Langford et al.

Title Page

Abstract

Introduction

Conclusions

References

Tables

Figures



Back

Close

Full Screen / Esc

Printer-friendly Version

Interactive Discussion



- Nemitz, E., Jimenez, J. L., Huffman, J. A., Ulbrich, I. M., Canagaratna, M. R., Worsnop, D. R., and Guenther, A. B.: An eddy-covariance system for the measurement of surface/atmosphere exchange fluxes of submicron aerosol chemical species – first application above an urban area, *Aerosol Sci. Tech.*, 42, 636–657, 2008.
- 5 Nemitz, E., Coyle, M., Langford, B., Gerosa, G., Marzuoli, R., Stella, P., Benjamin Loubet, B., Potier, E., Joensuu, J., Altimir, N., Ammann, C., Vuolo, R., Pilegaard, K., and Weidinger, T.: Eddy-covariance flux measurements of ozone deposition: review and development of a common methodology, in preparation to *Atmos. Meas. Tech. Discuss.*, 2015.
- 10 Park, J.-H., Goldstein, A. H., Timkovsky, J., Fares, S., Weber, R., Karlik, J., and Holzinger, R.: Eddy covariance emission and deposition flux measurements using proton transfer reaction – time of flight – mass spectrometry (PTR-TOF-MS): comparison with PTR-MS measured vertical gradients and fluxes, *Atmos. Chem. Phys.*, 13, 1439–1456, doi:10.5194/acp-13-1439-2013, 2013.
- 15 Rannik, Ü., Mammarella, I., Aalto, P., Keronen, P., Vesala, T., and Kulmala, M.: Long-term aerosol particle flux observations, Part I: Uncertainties and time-average statistics, *Atmos. Environ.*, 43, 3431–3439, 2009.
- Rannik, Ü., Haapanala, S., Shurpali, N. J., Mammarella, I., Lind, S., Hyvönen, N., Peltola, O., Zahniser, M., Martikainen, P. J., and Vesala, T.: Intercomparison of fast response commercial gas analysers for nitrous oxide flux measurements under field conditions, *Biogeosciences*, 20 12, 415–432, doi:10.5194/bg-12-415-2015, 2015.
- Rinne, J. and Ammann, C.: Disjunct eddy covariance method, in: *Eddy Covariance: a Practical Guide to Measurements and Data Analysis*, edited by: Aubinet, M., Vesala, T., and Papale, D., Springer, Dordrecht, Heidelberg, London, New York, 10, 291–306, 2012.
- 25 Rummel, U., Ammann, C., Gut, A., Meixner, F. X., and Andreae, M. O.: Eddy Covariance measurements of nitric oxide flux within an Amazonian rain forest, *J. Geophys. Res.*, 107, 8050, doi:10.1029/2001JD000520, 2002.
- Shurpali, N. J., Verma, S. B., Clement, R. J., and Billesbach, D. P.: Seasonal distribution of methane flux in a Minnesota peatland measured by eddy-correlation, *J. Geophys. Res.-Atmos.*, 98, 20649–20655, 1993.
- 30 Spirig, C., Neftel, A., Ammann, C., Dommen, J., Grabmer, W., Thielmann, A., Schaub, A., Beauchamp, J., Wisthaler, A., and Hansel, A.: Eddy covariance flux measurements of biogenic VOCs during ECHO 2003 using proton transfer reaction mass spectrometry, *Atmos. Chem. Phys.*, 5, 465–481, doi:10.5194/acp-5-465-2005, 2005.

Eddy-covariance data with low signal-to-noise ratio

B. Langford et al.

Title Page

Abstract

Introduction

Conclusions

References

Tables

Figures



Back

Close

Full Screen / Esc

Printer-friendly Version

Interactive Discussion



- Stella, P., Kortner, M., Ammann, C., Foken, T., Meixner, F. X., and Trebs, I.: Measurements of nitrogen oxides and ozone fluxes by eddy covariance at a meadow: evidence for an internal leaf resistance to NO_2 , *Biogeosciences*, 10, 5997–6017, doi:10.5194/bg-10-5997-2013, 2013.
- 5 Stull, R. B.: *An Introduction to Boundary Layer Meteorology*, Kluwer Academic Publishers, London, 1988.
- Taipale, R., Ruuskanen, T. M., and Rinne, J.: Lag time determination in DEC measurements with PTR-MS, *Atmos. Meas. Tech.*, 3, 853–862, doi:10.5194/amt-3-853-2010, 2010.
- Valach, A. C., Langford, B., Nemitz, E., MacKenzie, A. R., and Hewitt, C. N.: Seasonal trends in concentrations and fluxes of volatile organic compounds above central London, *Atmos. Chem. Phys. Discuss.*, 15, 6601–6644, doi:10.5194/acpd-15-6601-2015, 2015.
- 10 Wienhold, F. G., Welling, M., and Harris, G. W.: Micrometeorological measurement and source region analysis of nitrous-oxide fluxes from an agricultural soil, *Atmos. Environ.*, 29, 2219–2227, doi:10.1016/1352-2310(95)00165-U, 1995.
- 15 Wyngaard, J. C.: On surface-layer turbulence, in: *Workshop on Micrometeorology*, edited by: Haugen, D. A., American Meteorology Society, Boston, 109–149, 1973.

Eddy-covariance data
with low
signal-to-noise ratio

B. Langford et al.

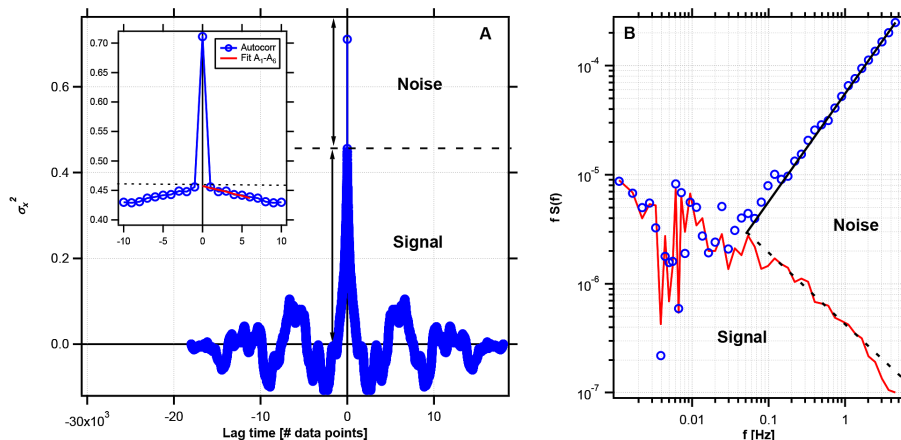


Figure 1. Illustration of the two methods for determination of analyser variance attributable to unstructured white noise, though **(a)** the use of an auto-covariance function and **(b)** from the variance power spectra in the frequency domain. The inset plot in **(a)** shows how the first few points of the auto-covariance function can be used to extrapolate the contributions of signal and noise components at a lag of zero.

Eddy-covariance data
with low
signal-to-noise ratio

B. Langford et al.

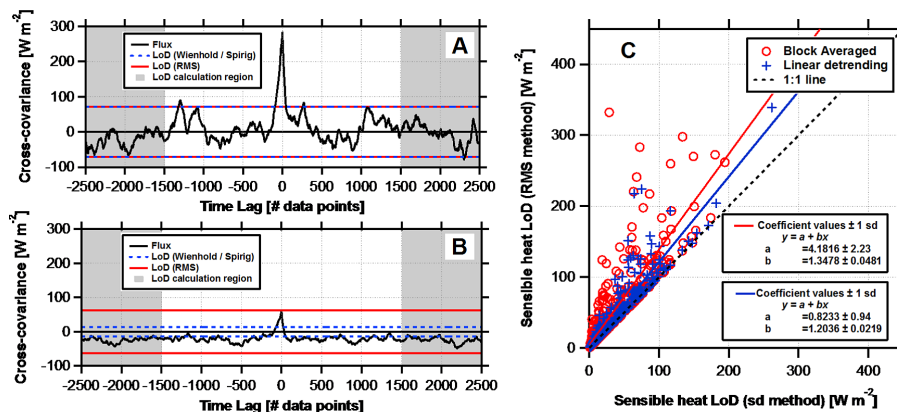


Figure 2. Cross-covariance functions for sensible heat fluxes (a and b) measured above a Douglas fir forest in Speuld, Netherlands, during two example measurement periods. (c) shows the limit of detection for sensible heat fluxes calculated either by block averaging or linearly detrending the vertical wind velocity and temperature data. The LoD were calculated using both the SD approach (Wienhold/Spirig) and the RMS approach. See text for further details.

Title Page

Abstract

Introduction

Conclusions

References

Tables

Figures

◀

▶

◀

▶

Back

Close

Full Screen / Esc

Printer-friendly Version

Interactive Discussion



Eddy-covariance data with low signal-to-noise ratio

B. Langford et al.

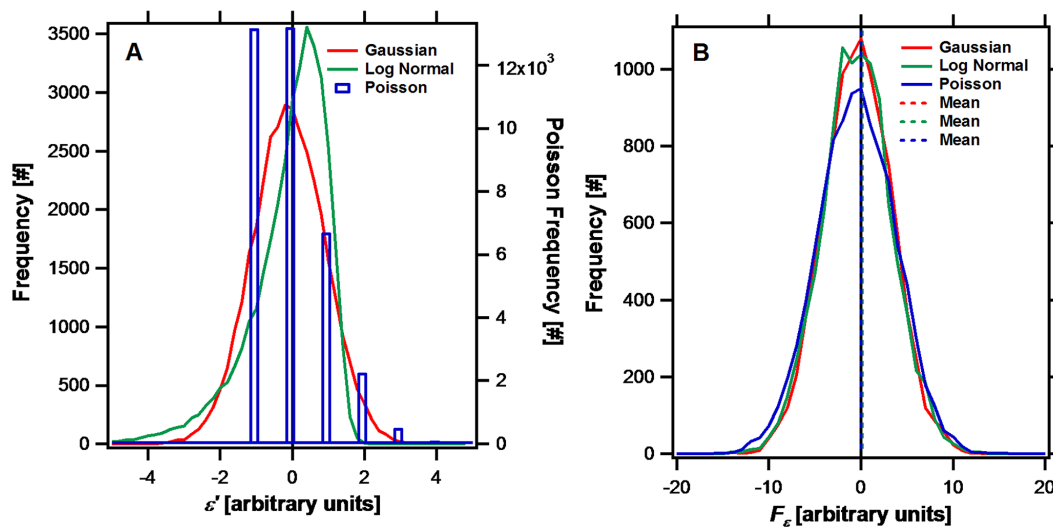


Figure 3. (a) shows the frequency distributions of Gaussian, log-normal and Poisson noise (ε') of identical SD. (b) shows the frequency distributions of the flux calculated from the unstructured white noise over a period of 5000 iterations. The mean average flux for each noise distribution are marked with dashed lines, which are all close to zero and consistently confirm that no systematic bias is introduced to a flux measurement regardless of the type of noise used.

Title Page

Abstract

Introduction

Conclusions

References

Tables

Figures

◀

▶

◀

▶

Back

Close

Full Screen / Esc

Printer-friendly Version

Interactive Discussion



**Eddy-covariance data
with low
signal-to-noise ratio**

B. Langford et al.

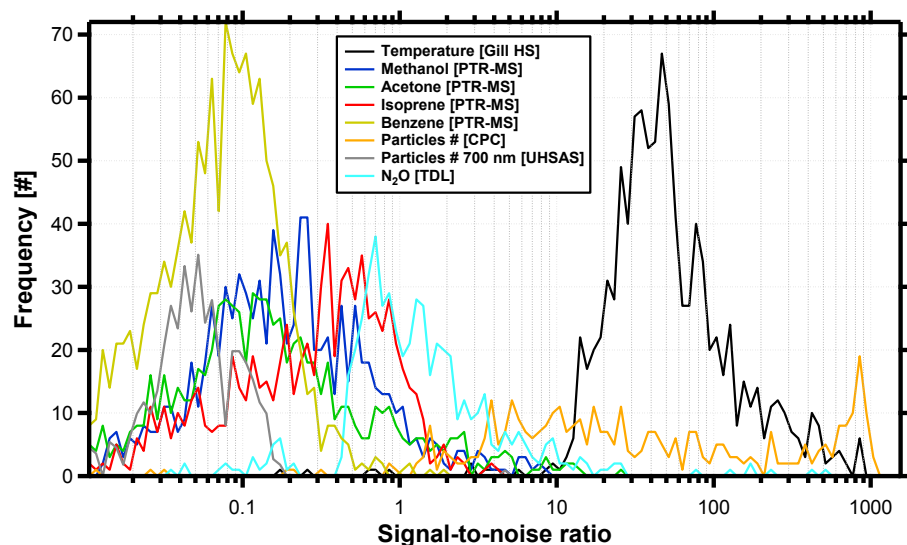


Figure 4. Signal-to-noise ratios of typical instruments used for the flux measurement of various trace gases and aerosols. Analysers include a sonic anemometer (temperature) and PTR-MS (isoprene, methanol and acetone) operated above a mixed Oak forest at a height of 32 m and above a city (benzene). Particle number concentrations were measured by a CPC and UHSAS (single size bin) above a Douglas fir forest and N₂O measurements were made above a grass land field in 2003 using the first generation of tuneable diode laser.

[Title Page](#)[Abstract](#)[Introduction](#)[Conclusions](#)[References](#)[Tables](#)[Figures](#)[Back](#)[Close](#)[Full Screen / Esc](#)[Printer-friendly Version](#)[Interactive Discussion](#)

Eddy-covariance data
with low
signal-to-noise ratio

B. Langford et al.

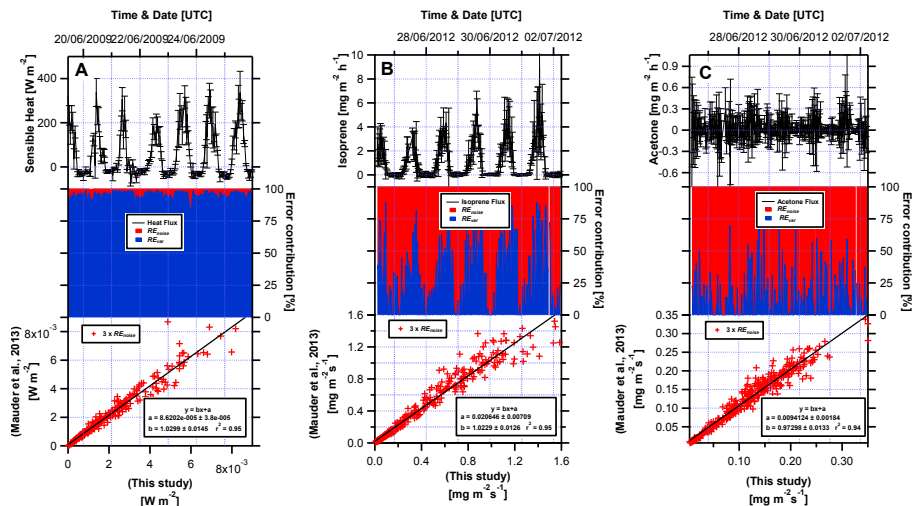


Figure 5. Sensible heat (a), isoprene (b) and acetone (c) fluxes and accompanying errors. Upper panels show the measured fluxes with error bars denoting the total random error (RE). The central panels show how the total random error can be divided errors associated with instrument noise (red, RE_{noise}) and the variability in turbulence at the genuine atmospheric concentration (blue, RE_{var}). The lower panels show scatter plots of the random instrument noise calculated using the analytical approximation of Mauder et al. (2013) and the numerical method outlined in this study.

Title Page

Abstract

Introduction

Conclusions

References

Tables

Figures



Back

Close

Full Screen / Esc

Printer-friendly Version

Interactive Discussion



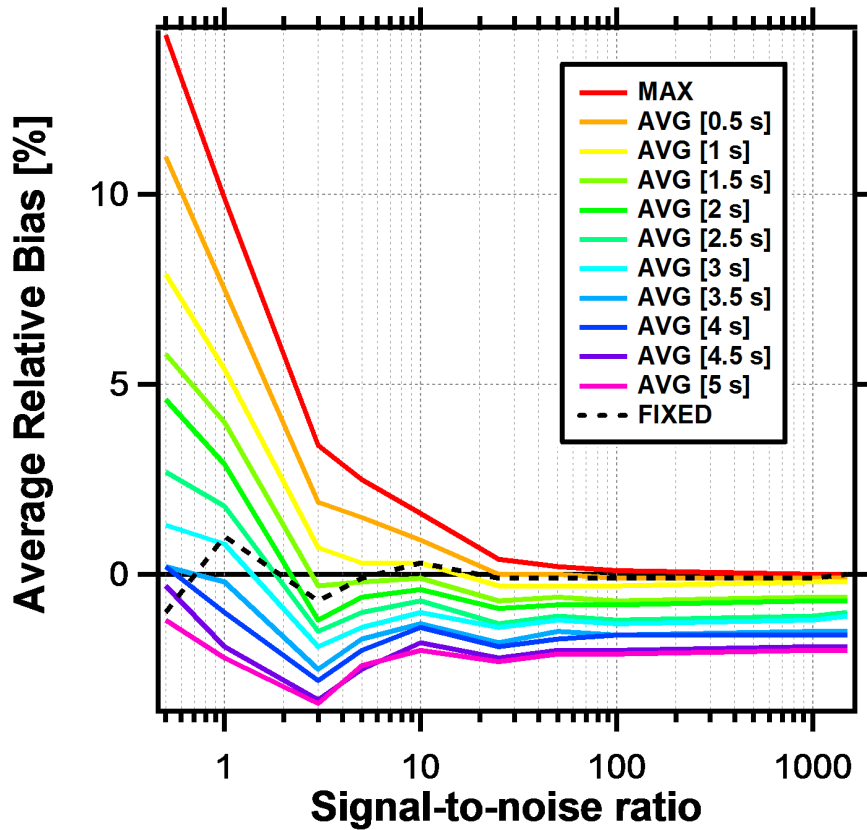


Figure 6. The average relative bias of a half-hourly flux as a function of the analyser signal-to-noise ratio for 31 days of 10 Hz eddy covariance sensible heat flux data acquired at a height of 32 m. The signal-to-noise ratio of the temperature data was deteriorated to match pre-defined limits. The errors shown are relative to the sensible heat flux calculated using the unmodified temperature data and a constant (0 s) time-lag.

Eddy-covariance data with low signal-to-noise ratio

B. Langford et al.

Title Page

Abstract Introduction

Conclusions References

Tables Figures

◀ ▶

◀ ▶

Back Close

Full Screen / Esc

Printer-friendly Version

Interactive Discussion



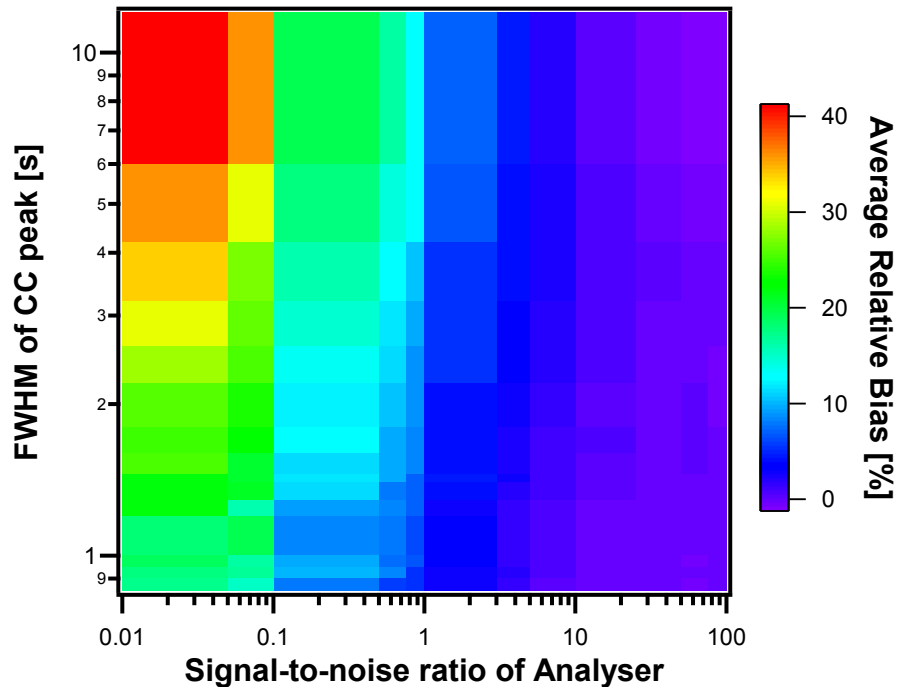


Figure 8. Image plot depicting the exponential relationship between the average relative bias and both the signal-to-noise ratio of the analyser and the full width half maximum (FWHM) of the cross-covariance function peak for simulated eddy covariance flux data calculated using the MAX time-lag method.

Eddy-covariance data with low signal-to-noise ratio

B. Langford et al.

Title Page

Abstract Introduction

Conclusions References

Tables Figures

◀ ▶

◀ ▶

Back Close

Full Screen / Esc

Printer-friendly Version

Interactive Discussion



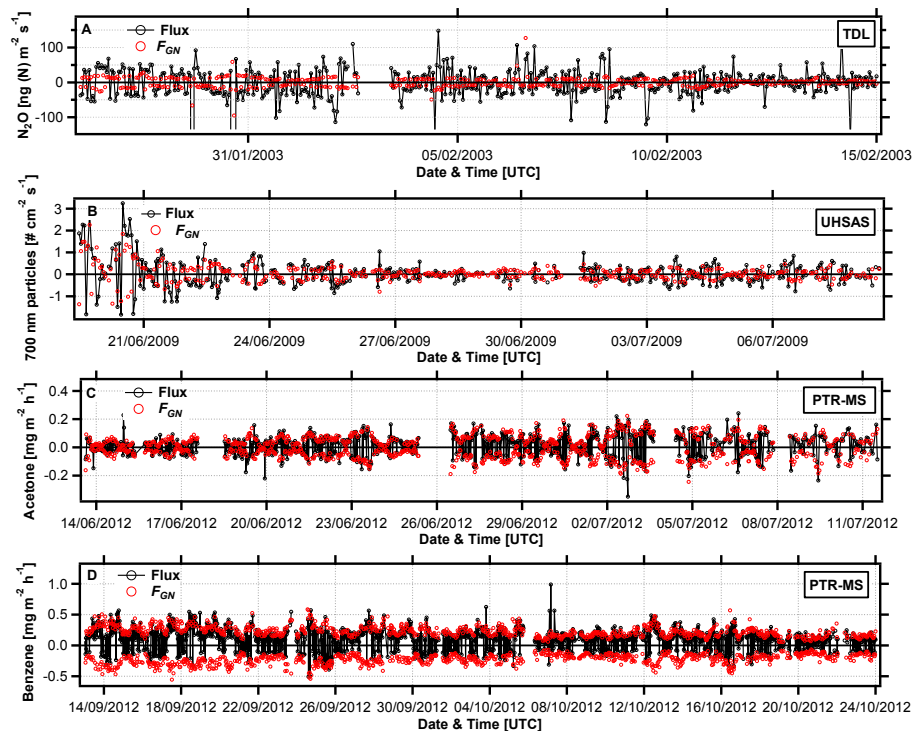


Figure 9. An example of “mirroring” in eddy covariance data with low SNR processed with the MAX time-lag method. The data were obtained by TDL (a), UHSAS (Data from a single size bin – b) and PTR-MS (c and d) instruments during four separate measurement campaigns. Red circles show a flux calculated from a Gaussian white noise time series based on the signal-to-noise ratio of the raw data and also calculated using the MAX time-lag method.

Eddy-covariance data with low signal-to-noise ratio

B. Langford et al.

Title Page	
Abstract	Introduction
Conclusions	References
Tables	Figures
◀	▶
◀	▶
Back	Close
Full Screen / Esc	
Printer-friendly Version	
Interactive Discussion	



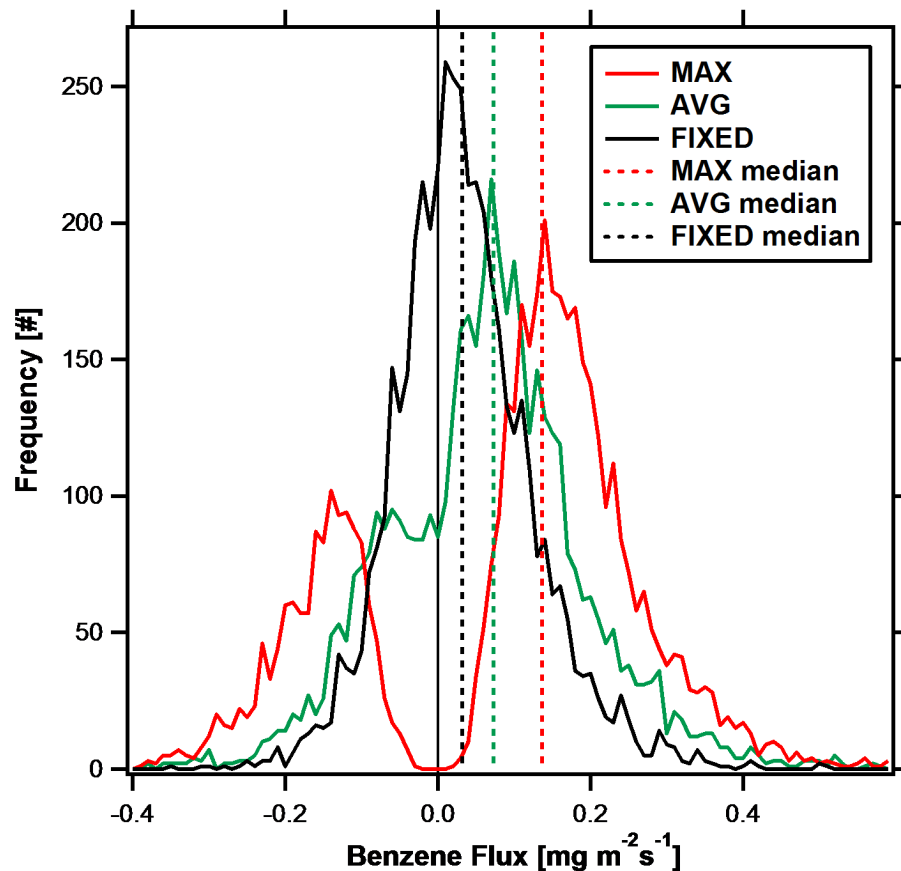


Figure 10. Distributions for benzene fluxes calculated using the MAX, AVG [5 s] and PRES time-lag methods. The data had an average signal-to-noise ratio of 0.09 and ranged between 0.007 and 0.24 at the 5th and 95th percentiles.

Eddy-covariance data with low signal-to-noise ratio

B. Langford et al.

Title Page

Abstract

Introduction

Conclusions

References

Tables

Figures

◀

▶

◀

▶

Back

Close

Full Screen / Esc

Printer-friendly Version

Interactive Discussion



Eddy-covariance data
with low
signal-to-noise ratio

B. Langford et al.

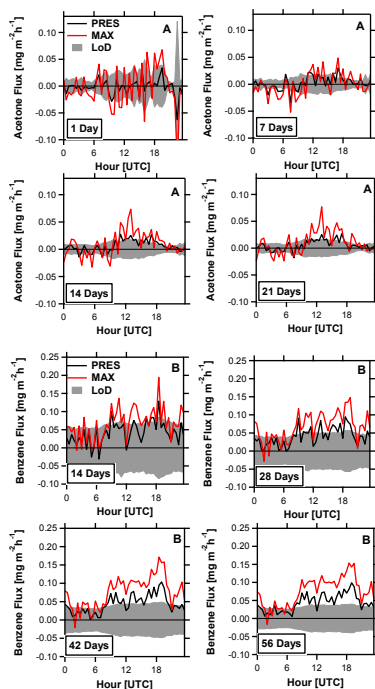


Figure 11. (a) Averaged diurnal profiles of acetone flux data obtained using a quadrupole PTR-MS. Increasing the number of data points averaged does not bring the PRES flux above the LoD (Greyed area indicating the LoD at the 95th percentile) indicating no detectable flux. By contrast, the MAX fluxes which are biased high, show some periods above the LoD which are an artefact of the MAX time-lag determination method. **(b)** Averaged diurnal profiles of benzene flux data obtained using a quadrupole PTR-MS. Increasing the number of data points averaged from 14 to 56 is sufficient to distinguish the flux calculated with a prescribed time-lag from the LoD (Greyed area indicating the LoD at the 95th percentile) and indicating a clear flux of benzene.

Title Page

Abstract

Introduction

Conclusions

References

Tables

Figures



Back

Close

Full Screen / Esc

Printer-friendly Version

Interactive Discussion



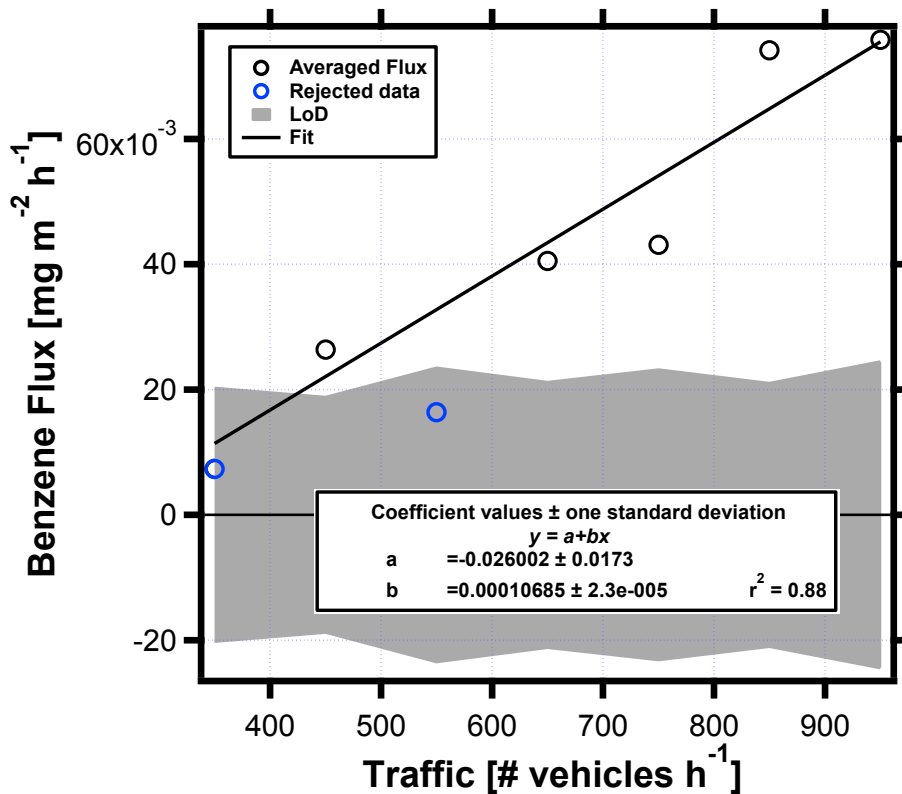


Figure 12. Benzene flux measurements calculated using a prescribed time-lag and averaged as a function of traffic density. Data points falling within the greyed area are down weighted in the fit as opposed to removing them completely which would bias the overall data set.

Eddy-covariance data with low signal-to-noise ratio

B. Langford et al.

Title Page

Abstract Introduction

Conclusions References

Tables Figures

◀ ▶

◀ ▶

Back Close

Full Screen / Esc

Printer-friendly Version

Interactive Discussion

